JOURNAL OF COMPUTATIONAL PHYSICS 24, 245–273 (1977)

Numerical Solutions for Viscous and Potential Flow about Arbitrary Two-Dimensional Bodies Using Body-Fitted Coordinate Systems*

FRANK C. THAMES,† JOE F. THOMPSON,‡ C. WAYNE MASTIN,§ AND RAY L. WALKER″

Department of Aerophysics and Aerospace Engineering, and Department of Mathematics, Mississippi State University, Mississippi State, Mississippi 39762

Received March 19, 1976; revised August 12, 1976

A procedure for numerical solution of the time-dependent, incompressible Navier–Stokes equations for the flow about arbitrarily shaped two-dimensional bodies is given. This solution is based on a technique of automatic numerical generation of a curvilinear coordinate system having a coordinate line coincident with the body contour regardless of its shape. The implicit solution utilizes the vorticity-stream function formulation with a false-position iterative adjustment of the surface vorticity in satisfaction of the no-slip boundary condition. All field equations are approximated using central differences and are solved simultaneously at each time step by SOR iteration. Excellent agreement with the Blasius boundary layer solution is obtained for a semi-infinite flat plate. Results are presented for Reynolds numbers up to 2000 for several airfoils and a cambered rock. A potential flow solution based on the same coordinate systems is also given, and excellent agreement with analytic solutions for Karman–Trefftz airfoils is shown.

1. INTRODUCTION

It is imperative in numerical solution of the Navier–Stokes equations that the boundary conditions be represented accurately in the finite-difference formulation, for the region in the immediate vicinity of solid surfaces is generally dominant in determining the character of the flow. The pressure and forces on solid bodies are directly dependent on the large gradients that prevail in this region near the surface, and accurate pressure and force coefficients require that these large gradients be represented accurately. This problem is accentuated at higher Reynolds numbers as the gradients become more severe.

Therefore, almost all numerical solutions of the Navier–Stokes equations generated to date have treated bodies for which a natural coordinate system is available, circles,

* Research sponsored by NASA–Langley Research Center, Grant NGR 25-001-055 and by Office of Naval Research, Contract N00014-74-C-0373.

† Engineering Specialist, Ph.D.; Present address: LTV Aerospace Corporation, Dallas, Texas.

‡ Professor of Aerophysics and Aerospace Engineering, Ph.D.

§ Associate Professor of Mathematics, Ph.D.

″ Graduate student, M.S.

ISSN 0021-9991

ellipses, spheres, Joukowski airfoils, and so forth. (Natural coordinate systems as defined here are those for which the body contour under consideration coincides with a constant coordinate line.) Mehta and Lavan [1] have given a solution about a modified Joukowski airfoil accomplished by generating a coordinate system with a conformal Joukowski transformation and solving the Navier–Stokes equations on the system. The basic Joukowksi transformation was modified somewhat by rounding the trailing edge and contracting the coordinates near the body. The method is limited to those bodies which can be generated by the Joukowski transformation (symmetric and cambered Joukowski airfoils, flat plates, and circular and elliptic cylinders, etc.).

Arbitrary two-dimensional bodies have not been successfully attacked as yet, primarily because of the difficulty of accurate representation of the boundary conditions and the large gradients near solid surfaces when no coordinate line is coincident with the body contour. Some solutions have been attempted with interpolation between grid points for boundaries not coincident with coordinate lines, but this necessarily introduces irregularity into an otherwise smooth boundary and places the most inaccurate difference representation in precisely the region of greatest sensitivity. Dawson and Marcus [2] attempted to create a method for general bodies by the use of two uniform rectangular grids: a fine inner grid surrounding the body and extending for perhaps one characteristic body dimension, and a coarse outer grid surrounding the inner grid and extending outward for perhaps 10 to 12 body diameters. The two grids overlap to allow for accurate transition between the two mesh systems. Only a circular cylinder solution was attempted, and this solution was restricted to small Reynolds numbers ($R \leqslant 1000$) because of boundary instabilities.

Recently, Meyder [3] presented a solution for the flow in a rod bundle using orthogonal curvilinear coordinates generated by solving for the potential and "force" lines in a simply-connected region and taking these as the coordinate lines. The solution for the curvilinear coordinates was done, however, on a rectangular grid using interpolation. Finally, Gal-Chen and Somerville [4, 5] have given a generalized formulation of the Navier–Stokes equations for a nonorthogonal coordinate system and developed a numerical solution for the flow in a simply-connected region having an irregular boundary, with application to the flow over mountainous terrain.

Numerical incompressible potential flow solutions for bodies of arbitrary shape have generally fallen into three categories.

(1) Integral equation methods, whereby various singular solutions of Laplace's equation are superposed to construct a solution satisfying the boundary conditions of the particular problem of interest. This type of aproach is represented by the work in Refs. [6–12]. In these methods singular solutions of Laplace's equation are distributed on the body surface, and perhaps also in its interior, with the body surface represented by quadralateral or triangular panels. The strengths of the singularities are then determined such that the superposition of the onset velocity field and that induced by the totality of the singularities satisfies the condition of vanishing normal velocity at the body surface at certain points. This approach has been carried to a high

degree of refinement and is presently capable of treating the flow about multiple bodies of arbitrary shape. This procedure obviates calculation in the entire flow field and involves instead the solution of a matrix equation of order equal to the number of points of application of the boundary condition on the bodies. The primary output is the surface pressure distribution on the bodies and the resulting aerodynamic coefficients. The velocity field can also be obtained, but this requires the evaluation of the velocity at each point in the field from a summation over all the singularities involved, a time consuming process. The determination of streamlines, or equivalently the stream function, from the velocity field is still another numerical problem itself.

(2) Finite element methods, as represented by Refs. [13–15]. Here the calculation is carried out in the entire flow field, the field being divided into finite elements. The flow solution is obtained by applying an integral variational principle, or other integral relations, over the aggregate of elements, which leads to a matrix solution of order equal to the total number of elements in the field. The solution is thus obtained in the entire flow field. However, not all derivatives can be made continuous across the boundaries between the various elements.

(3) Conformal transformation, whereby the field is transformed to one of simple geometry on which the solution is known (two-dimensional flow only). The classic Theodorsen method [16] is one of this type. A comparative discussion of earlier applications of this and other procedures is given in [6]. Recently Ives [17] has extended this approach to multiple bodies.

Finite-difference solutions have been severly hindered in the past by the problem of fitting curved boundaries into the computational grid. The use of interpolation between grid points to represent boundary conditions on a curved boundary passing through a rectangular grid may lead to poor application of the boundary conditions. Since finite-difference solutions depend on continuity of derivatives, the distribution of points at will in the field leads to difference expressions involving large numbers of points, loss of repeat patterns over the field, and hence unreasonably complex computer codes.

However, if a curvilinear coordinate system with coordinate lines coincident with the field boundaries can be found, these problems vanish, and the finite-difference approach can give very smooth solutions that do not lack continuity of derivatives. The flow solutions reported herein are based on just such an approach.

The automatic numerical generation of a general curvilinear coordinate system with coordinate lines coincident with all boundaries of a general multiconnected region containing any number of arbitrarily shaped bodies should alleviate the problem of arbitrary bodies with these and other partial differential systems [18]. In this procedure, the curvilinear coordinates are generated as the solution of two elliptic partial differential equations with Dirichlet boundary conditions, one coordinate being specified to be constant on each of the boundaries, and a distribution of the other being specified along the boundaries. This general idea has been applied

previously to two-dimensional regions interior to a closed boundary (simply-connected regions) by Winslow [19], Barfield [20], Chu [21], Amsden and Hirt [22], and Godunov and Prokopov [23]. Winslow [19] and Chu [21] took the transformed coordinates to be solutions of Laplace's equation in the physical plane which, as is shown in the next section, makes the physical cartesian coordinates solutions of a quasi-linear elliptic system in the transformed plane. Barfield [20] and Amsden and Hirt [22] reversed the procedure, taking the physical coordinates to be solutions in the transformed plane of a linear elliptic system which consists of Laplace's equation modified by a multiplicative constant on one term. This makes the transformed coordinates solutions of a quasi-linear elliptic system in the physical plane. Barfield also considered a hyperbolic system, but such a system cannot be used to treat general closed boundaries, since only elliptic systems allow specification of boundary conditions on the entirety of closed boundaries. Stadius [24] also used a hyperbolic system to generate a coordinate system for a doubly-connected region having parallel inner and outer boundaries. With parallel boundaries it is only necessary to specify conditions on one of the boundaries, the location of the other boundary being free. The elliptic system, however, allows all boundaries to be specified as desired and thus has much greater flexibility.

Amsden and Hirt [22] constructed the coordinate generation method by iterative weighted averaging of the values of the physical coordinates at fixed points in the transformed plane in terms of values at nieghboring points. Although not stated as such, this procedure is precisely equivalent to solving Laplace's equation, or modification thereof of the form noted above in Barfield [20], for the physical coordinates in the transformed plane by Gauss–Seidel iteration. Amsden and Hirt also allowed the boundary to move at each iteration, but this is simply equivalent to approaching the solution of the boundary-value problem through a succession of boundary-value problems converging to the problem of interest. In the approach of Godunov and Prokopov [23] the elliptic system is quasi-linear in both the physical and transformed planes. These authors applied a second transformation to that used by Chu [21], the transformation functions of this latter transformation being chosen a priori to control the coordinate spacing. Though not stated as such, the overall transformation may be shown to be generated by taking the transformed coordinates to be solutions in the physical plane of Laplace's equation modified by the addition of a multiple of the square of the Jacobian, the multiplicative factors being a priori chosen functions of the physical coordinates.

Meyder [3] generated an orthogonal curvilinear system by solving for the potential and "force" lines in a simply-connected region and taking these as the coordinate lines. This amounts to making the curvilinear coordinates solutions of Laplace equations in the physical plane with Dirichlet boundary conditions (constant) on part of the boundary and Neumann boundary conditions (vanishing normal derivative) on the remainder. The solution for the coordinates was done, however, in the physical plane on a rectangular grid using interpolation at the curved boundaries, rather than in the transformed plane.

In the present research, the technique of generating the transformed coordinates as

solutions of an elliptic differential system in the physical plane has been applied to multiconnected regions with any number of arbitrarily shaped bodies (or holes). The elliptic equations for the coordinates are solved in finite-difference approximation by successive overrelaxation (SOR) iteration. Coordinate lines may be concentrated as desired along the boundaries. Spacing of the coordinate lines encircling the body may be controlled by adjusting parameters in the partial differential equations for the coordinates.

Regardless of the shape and number of the bodies and regardless of the spacing of the curvilinear coordinate lines, all numerical computations, both to generate the coordinate system and subsequently to solve partial differential equaitons on the coordinate system, are done on a rectangular grid with a square mesh, that is, in the transformed plane. It is also possible to cause the coordinate system to change in time as desired and still have all computation done on a fixed rectangular grid with square mesh. This allows the curvilinear coordinate system in the physical plane to deform with a deforming body, blast front, shock, free surface, or any other boundary, keeping a coordinate line always coincident with the boundary at all times. The physical coordinate system has been in effect, eliminated from the problem, at the expense of adding two elliptic equations to the original system.

Since the curvilinear coordinate system has coordinate lines coincident with the surface contours of all bodies present, all boundary conditions may be expressed at grid points. Also, normal derivatives on the bodies may be represented by using only finite differences between grid points on coordinate lines, without need of any interpolation, even though the coordinate system is not orthogonal at the boundary. Numerical solutions for the lifting and nonlifting potential flow about Karman–Trefftz airfoils obtained with this coordinate system generation show excellent comparison with the analytic solutions.

This method of automatic body-fitted curvilinear coordinate generation has been used to construct a finite-difference solution of the full, incompressible, time-dependent Navier–Stokes equations for the laminar viscous flow about arbitrary two-dimensional airfoils or any other two-dimensional body [25]. The Navier–Stokes equations are written in the vorticity-stream function formulation, with the vorticity on the body being determined by a type of false-position iteration so that the no-slip boundary condition is satisfied. The solution is implicit in time, the vorticity and the stream function equations being solved simultaneously at each time step by SOR iteration. A method of controlling the spacing of the coordinate lines encircling the body has been developed in order to treat high Reynolds number flow, since the coordinate lines must concentrate near the surface to a greater degree as the Reynolds number increases. The solution is designed to provide the velocity field, the surface pressure distribution, and the lift, drag, and moment coefficients. Initial application to multiple airfoils has also been made [26]. Results are given for separated flow over several airfoils and an arbitrary rock. A comparison with the Blasius flat plate boundary layer solution is also given.

2. Body-Fitted Coordinate Systems

A. *Mathematical Development*

The basic approach of constructing body-fitted curvilinear coordinates in general multiconnected regions as the solution of an elliptic boundary-value problem has been covered by the authors in previous publications [18, 25, 28]. A detailed report of the technique, together with examples, the computer code, and a users' manual, is now available [28]. The technique of application to the numerical solution of partial differential equations is also illustrated therein.

Consider transforming the two-dimensional, doubly-connected region D, bounded by two, simple, closed, arbitrary contours, Γ_1 and Γ_2, onto a rectangular region, D^*, as illustrated in Fig. 1. We require that Γ_1 map onto $\Gamma_1{}^*$, Γ_2 onto $\Gamma_2{}^*$, Γ_3 onto $\Gamma_3{}^*$, and Γ_4 onto $\Gamma_4{}^*$. Note that $\Gamma_1{}^*$ and $\Gamma_2{}^*$ are required to be constant η-lines, while the arbitrary cut between contours Γ_1 and Γ_2 (i.e., Γ_3 and Γ_4) becomes constant

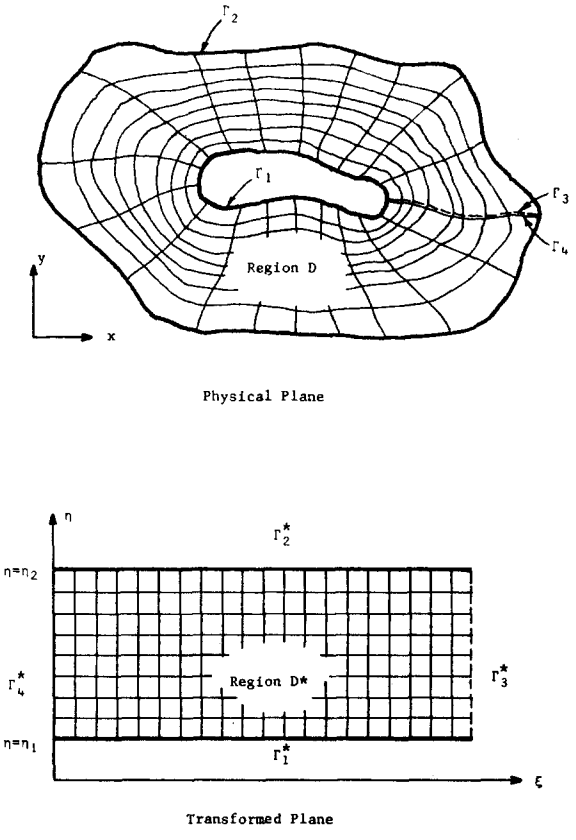

FIG. 1. Field transformation—Single body.

ξ-lines. The region D is the physical plane, D^* the transformed plane, Γ_1 the body contour, and Γ_2 the remote boundary contour.

As discussed previously, the curvilinear coordinates are generated by solving an elliptic system of the form

$$\xi_{xx} + \xi_{yy} = P(\xi, \eta), \tag{1a}$$

$$\eta_{xx} + \eta_{yy} = Q(\xi, \eta), \tag{1b}$$

with Dirichlet boundary conditions, one coordinate being specified to be equal to a constant on the body and equal to another constant on the outer boundary, with the other coordinate varying monotonically over the same range around both the body and the outer boundary. (See [25, 27], or [28] for more detail.)

Since it is desired to perform all numerical computations in the uniform rectangular transformed plane, the dependent and independent variables must be interchanged in Eq. (1). This results in the coupled system (see [28] for the transformation relations)

$$\alpha x_{\xi\xi} - 2\beta x_{\xi\eta} + \gamma x_{\eta\eta} = -J^2[x_\xi P(\xi, \eta) + x_\eta Q(\xi, \eta)], \tag{2a}$$

$$\alpha y_{\xi\xi} - 2\beta y_{\xi\eta} + \gamma y_{\eta\eta} = -J^2[y_\xi P(\xi, \eta) + y_\eta Q(\xi, \eta)], \tag{2b}$$

where

$$\alpha = x_\eta^2 + y_\eta^2, \qquad \gamma = x_\xi^2 + y_\xi^2,$$

$$\beta = x_\xi x_\eta + y_\xi y_\eta, \qquad J = x_\xi y_\eta - x_\eta y_\xi,$$

The system described by Eq. (2) is a quasi-linear elliptic system for the coordinate functions $x(\xi, \eta)$ and $y(\xi, \eta)$ in the transformed plane. This set is considerably more complex than the linear system specified by Eq. (1), but the boundary conditions are specified on straight boundaries, and the coordinate spacing in the transformed plane is uniform. The inhomogeneous functions $P(\xi, \eta)$ and $Q(\xi, \eta)$ are sums of decaying exponentials [28] that allow coordinate lines to be attracted to specified lines and/or points in the field or on the boundaries as discussed in more detail in [28].

The method can also be applied to regions containing any number of arbitrary bodies and to regions with time-dependent boundaries. Discussions of these techniques are given in [26–28].

B. *Numerical Implementation*

The transformed field for a single airfoil is illustrated in Fig. 2. The physical coordinates of I points describing the body surface, (x, y), provide the boundary conditions along the $j = 1$ line, and those of I points on the physical remote boundary, usually a circle of radius ten or more chords, supply the boundary conditions along the $j = J$ line of the transformed field. Since the side boundaries of the transformed field are reentrant, corresponding to the cut in the physical plane, we have $f_{I,j} = f_{1,j}$ and $f_{I+1,j} = f_{2,j}$ for all j. Note that the values of x and y are not specified on these side boundaries. All derivatives in (2) are approximated by second-order central difference

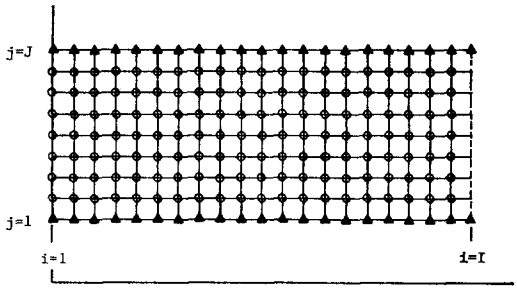

FIG. 2. Computational grid.

expressions ($\Delta\xi$ and $\Delta\eta$ are both unity by construction, the actual values of ξ and η being immaterial since cancellation occurs after substitution in the transformed equations).

$$
\begin{aligned}
(f_\xi)_{ij} &\cong \tfrac{1}{2}(f_{i+1,j} - f_{i-1,j}),\\
(f_\eta)_{ij} &\cong \tfrac{1}{2}(f_{i,j+1} - f_{i,j-1}),\\
(f_{\xi\xi})_{ij} &\cong f_{i+1,j} - 2f_{ij} + f_{i-1,j},\\
(f_{\eta\eta})_{ij} &\cong f_{i,j+1} - 2f_{ij} + f_{i,j-1},\\
(f_{\xi\eta})_{ij} &\cong \tfrac{1}{4}(f_{i+1,j+1} - f_{i+1,j-1} - f_{i-1,j+1} + f_{i-1,j-1}).
\end{aligned}
$$

The resulting set of $2I(J-1)$ nonlinear difference equations, two for each point (i, j) for $i = 1, 2, \ldots, I-1$ and $J = 2, 3, \ldots, J-1$, are solved by accelerated Gauss–Seidel (SOR) iteration using overrelaxation. The iteration is considered to have converged when the maximum absolute change on the field between iterates is less than a specified value. A range of acceleration parameters was examined, and a value of 1.85 was nearly optimum for the airfoils considered. After convergence of the solution of (2), the values of the coefficients α, β, γ, J, at each point of the field are stored for use in the solution of the partial differential equations.

3. NAVIER–STOKES EQUATIONS

A. *Mathematical Formulation*

1. *Basic equations.* The stream function-vorticity formulation of the two-dimensional, incompressible viscous flow equations is given by

$$\omega_t + \psi_y\omega_x - \psi_x\omega_y = (\omega_{xx} + \omega_{yy})/R, \tag{3a}$$

$$\psi_{xx} + \psi_{yy} = -\omega, \tag{3b}$$

where ψ is the nondimensional stream function, ω the nondimensional vorticity, and R is the Reynolds number based on the characteristic velocity (freestream value) and body length. The set (3) is in the nonconservative formulation. Equations (3)

may be transformed utilizing the operations given in [28], yielding the set applicable in the rectangular transformed plane. The transformed equations are

$$\omega_t + (\psi_\eta\omega_\xi - \psi_\xi\omega_\eta)/J = (\alpha\omega_{\xi\xi} - 2\beta\omega_{\xi\eta} + \gamma\omega_{\eta\eta})/J^2R + (Q\omega_\eta + P\omega_\xi)/R, \quad (4a)$$

$$(\alpha\psi_{\xi\xi} - 2\beta\psi_{\xi\eta} + \gamma\psi_{\eta\eta})/J^2 + Q\psi_\eta + P\psi_\xi = -\omega, \quad (4b)$$

with boundary conditions

$$\psi = \psi_0 = \text{constant}, \qquad \gamma^{1/2}\psi_\eta/J = 0, \qquad [\xi, \eta_1] \in \Gamma_1^*, \quad (4c)$$

$$\psi = y(\xi, \eta_2)\cos\theta - x(\xi, \eta_2)\sin\theta, \qquad \omega = 0, \qquad [\xi, \eta_2] \in \Gamma_2^*, \quad (4d)$$

where θ is the angle of attack. The second of (4c) guarantees that the no-slip condition is satisfied on the body surface. The satisfaction of this condition is accomplished by iteratively adjusting the value of the vorticity on the body surface, utilizing a false-position procedure, until the second-order forward difference approximation to the velocity component tangential to the body surface, $V_{\tau_\eta} = \gamma^{1/2}\psi_\eta/J$, is below some tolerance. The iterative algorithm is given by

$$\omega_{i,1}^{(k+1)} = \omega_{i,1}^{(k)} - \delta\,\frac{\omega_{i,1}^{(k)} - \omega_{i,1}^{(k-1)}}{(V_{\tau_\eta})_{i,1}^{(k)} - (V_{\tau_\eta})_{i,1}^{(k-1)}}\,(V_{\tau_\eta})_{i,1}^{(k)} \quad (5)$$

where k denotes iteration count, δ an adjustable parameter, and $(i, 1)$ refers to some point on the body surface. This method is an extension of an approach suggested by Israeli [29].

2. *Pressure coefficients.* Pressure coefficients on the body surface are obtained by the line integral method as follows. If the primitive variable form of the Navier–Stokes equations is evaluated on the body surface, the velocity time derivative and the inertia terms vanish yielding

$$\nabla P = \nabla^2\mathbf{V}/R \quad (6)$$

where the quantities are nondimensional in the usual fashion. Using a vector identity to eliminate the Laplacian of the velocity, dotting this equation with $d\mathbf{r}$ (an arc length differential along the body contour Γ_1), and transforming produces

$$dP = (1/RJ)(\beta\omega_\xi - \gamma\omega_\eta)\,d\xi, \quad (7)$$

Integration along the transformed body contour, Γ_1^*, yields

$$C_p^*(\xi) = P(\xi) - P_{\text{T.E.}} = (1/R)\int_{\xi_{T.E.}}^{\xi} (1/J)(\beta\omega_\xi - \gamma\omega_\eta)\,d\xi'. \quad (8)$$

3. *Force coefficients.* If body forces are neglected, the force on a body immersed in a moving viscous fluid is determined by integrating the stress vector, $\mathbf{T}$, over the body surface

$$\mathbf{F} = C_A\mathbf{i} + C_n\mathbf{j} = \int_S \mathbf{T}\,dS$$

where S is the body surface. Substituting for T [30], and using the transformations given in [28],

$$C_D = 2\int_{\xi_{min}}^{\xi_{max}} (y_\xi \cos\theta - x_\xi \sin\theta)\, C_p^*\, d\xi - 2\int_{\xi_{min}}^{\xi_{max}} (y_\xi \sin\theta + x_\xi \cos\theta)(\omega/R)\, d\xi, \tag{9a}$$

$$C_L = -2\int_{\xi_{min}}^{\xi_{max}} (x_\xi \cos\theta + y_\xi \sin\theta)\, C_p^*\, d\xi + 2\int_{\xi_{min}}^{\xi_{max}} (x_\xi \sin\theta - y_\xi \cos\theta)(\omega/R)\, d\xi. \tag{9b}$$

The two integrals in (9a) are referred to as the pressure and friction drag coefficients and are denoted C_{D_P} and C_{D_F}, respectively.

B. *Numerical Produres*

1. *Difference equations.* The basic equations (4a), (4b) with boundary conditions (4c), (4d), and (5) were solved numerically with the fully implicit, backward-time, central-space formulation (BTCS). A two-point, first-order backward difference was used to approximate the time derivative, while second-order central differences were employed for the spatial derivatives. Point SOR iteration was employed to converge the elliptic space variation of Eqs. (4). The integration in Eqs. (8) and (9) was performed with the trapezoidal rule. Derivatives appearing in these relations were calculated using second-order forward (η-derivatives) or central (ξ-derivatives) approximations.

2. *Convergence acceleration.* Special procedures were used to evaluate the relaxation factors for both the stream function and vorticity transport equations. If the cross derivative terms in (4a), (4b) are neglected (β is generally small), it is possible to calculate optimum SOR acceleration parameters at each point of the computational net [28]. Since the ψ-equation is linear, the optimum parameter is constant over the mesh and was found to be about 1.85. However, the vorticity equation is quasi-linear, and thus the optimum parameter should vary over the field. In particular since the ψ_ξ and ψ_η derivatives are small near the body, Eq. (4a) assumes a Poisson character in this region. Poisson equations characteristically have optimum relaxation factors greater than unity. Conversely, as the radial distance from the body increases, the viscous diffusion terms become negligible and the convection terms dominate. Under these conditions a parameter less than unity is optimum for the ω-equation. The above discussion indicates the feasibility of varying the vorticity equation acceleration parameter over the computational field. This approach was tried with some success with the Karman–Trefftz airfoils. For these bodies it was found that the optimum parameter varied linearly with η from a value of 1.4 immediately adjacent to the body to a value of 0.9 at the twentieth η-line. Parameters in the remainder of field were essentially constant with a value of 0.9 for the Reynolds numbers considered.

3. *Stability.* Although the stability of the implicit BTCS method for linear parabolic equations is unlimited, this is not the case with nonlinear difference equations. However, such approaches do significantly broaden the available time step envelope. The solutions documented in the current paper utilized small time steps ($\Delta t = O(2/R)$) in the initial phases to damp the effects of the impulsive start. Time steps were subsequently increased to values of the order of $10/R$ to $20/R$ without significant increases in the number of iterations required to converge each step.

4. *Computer time.* All solutions were run on the UNIVAC 1106 system. It is difficult, if not impossible, to draw any consistent and general conclusions regarding the computer time requirements of the viscous flow solutions. Problem variables having significant impact on computation time include angle of attack, Reynolds number, time step, computational method, convergence criteria, field size, and body geometry. As an indication of how difficult it is to develop a correlation of CPU requirements based on the above-stated variables, consider a comparison of the flapped Karman–Trefftz and Göttingen 625 airfoil solutions. Although the Göttingen solution was run at ten times the Reynolds number with a field size 12% larger, the time required to converge a comparable-sized time step was roughly one-half of that required for the flapped Karman–Trefftz airfoil. Convergence of this latter solution was slowed by difficulties with the boundary vorticity iteration near the airfoil trailing edge. However, on the average, the airfoil and rock solutions required approximately 4 min per time step for nominal field sizes of 4000. For the computational methods used, improved CPU times would result primarily from an improved numerical algorithm for the body vorticity calculations.

C. *Results*

Viscous flows about a finite flat plate and five different bodies were calculated using the numerical procedures outlined above [25]. These bodies included a circular cylinder, cambered and flapped Karman–Trefftz airfoils, a Göttingen 625 airfoil, and the Cambered Rock. Reynolds numbers of the flows about the bodies ranged from 200 to 2000 at angles of attack from 0 to 15 degrees. The results of these numerical flow simulations are summarized below.

1. *Semi-infinite flat plate solution.* This numerical solution of the full Navier–Stokes equations was applied to the development of the flow over a semi-infinite flat plate [31] in order to test the use of the boundary-fitted coordinate systems for viscous flow solutions. All quantities are nondimensionalized with respect to the freestream velocity and unit length. The Reynolds number, R, is defined in terms of these reference values. The transformation from the physical to the transformed field is indicated schematically in Fig. 3. The coordinate system was generated as the solution of (2) with boundary conditions as follows:

on $a'b'$ (plate surface): $x =$ specified as desired, $y = 0$.
on $a'c'$ (upper boundary): $x =$ specified as desired, $y = 10(x/R)^{1/2}$.
on $b'c'$ (downstream boundary): $x =$ constant, $y =$ specified as desired.
on $a'a'$ (leading edge): $x = y = 0$.

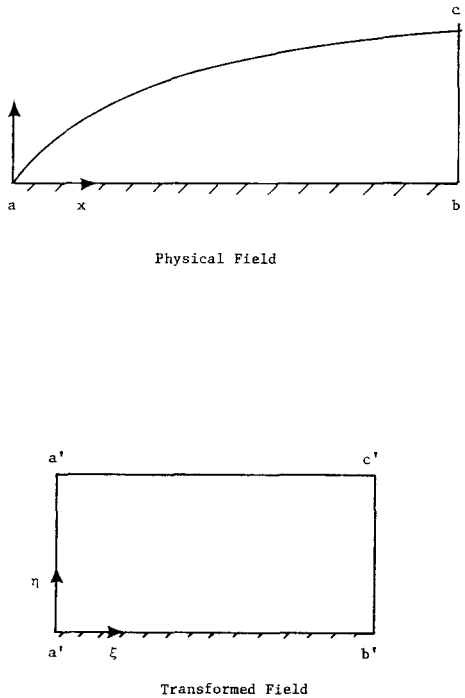

FIG. 3. Relation between physical and transformed fields—Semi-infinite flat plate.

The condition on y on the upper boundary, $a'c'$, places this boundary at twice the Blasius boundary layer thickness [32]. The downstream boundary was located at multiples of the distance at which the slope of the Blasius boundary layer is 0.01.

The boundary conditions for the Navier–Stokes equations in the transformed plane are as follows:

on $a'b'$ (plate surface): $\psi = \psi_\eta = 0$ ($v = u = 0$, no-slip condition).

on $a'c'$ (upper boundary): $\psi_\eta = (1/x_\xi)(J + x_\eta \psi_\xi)$, $\omega = 0$ ($u = 1$, $\omega = 0$, freestream conditions).

on $b'c'$ (downstream boundary):

$$\psi = 2(t/R)^{1/2} \int_0^{\eta/2(t/R)^{1/2}} \operatorname{erf} \eta \, d\eta,$$

$$\omega = -(R/\pi t)^{1/2} \exp(-(Ry^2/4t)) \qquad \text{(infinite plate solution, Schlichting [32])}$$

on $a'a'$ (leading edge): $\psi = \omega = 0$.

The condition on the downstream boundary, $b'c'$, is the exact solution of the Navier–Stokes equations for a suddenly accelerated fully infinite flat plate. The numerical quadrature was done by trapezoidal integration. The condition on ψ_η

on the upper boundary expresses $u = 1$, the freestream velocity. All these boundary conditions were implemented directly except the $\psi_\eta = 0$ condition on the plate, $a'b'$, which was satisfied by adjusting the value of the vorticity at each point on the body by the false-position iteration procedure discussed above.

The coordinate system used for the semi-infinite plate, shown in Fig. 4 has a curved boundary located at twice the Blasius boundary layer thickness above the plate, with coordinate lines coming to a point at the leading edge. This form was chosen in preference to systems with rectangular boundaries in order to concentrate the coordinate lines near the plate to a greater degree as the Reynolds number increases and also to ensure a test of a representative nonorthogonal curvilinear system.

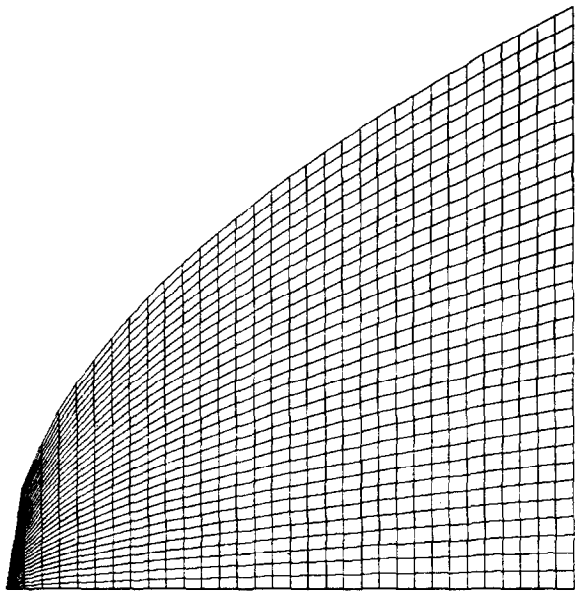

(a). Vertical Scale Exaggerated for Plot

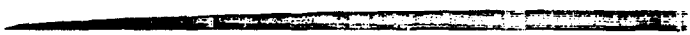

(b). Actual System

FIG. 4. Coordinate system—Semi-infinite flat plate.

Velocity profiles obtained using this coordinate system are shown in Fig. 5 and compared therein with the Blasius boundary layer solution (Schlichting [32]). (Positions are given in fractions of the distance to the downstream boundary.) Since the downstream boundary condition was the time-dependent solution for the completely infinite plate, for which the boundary layer thickness increases without bound

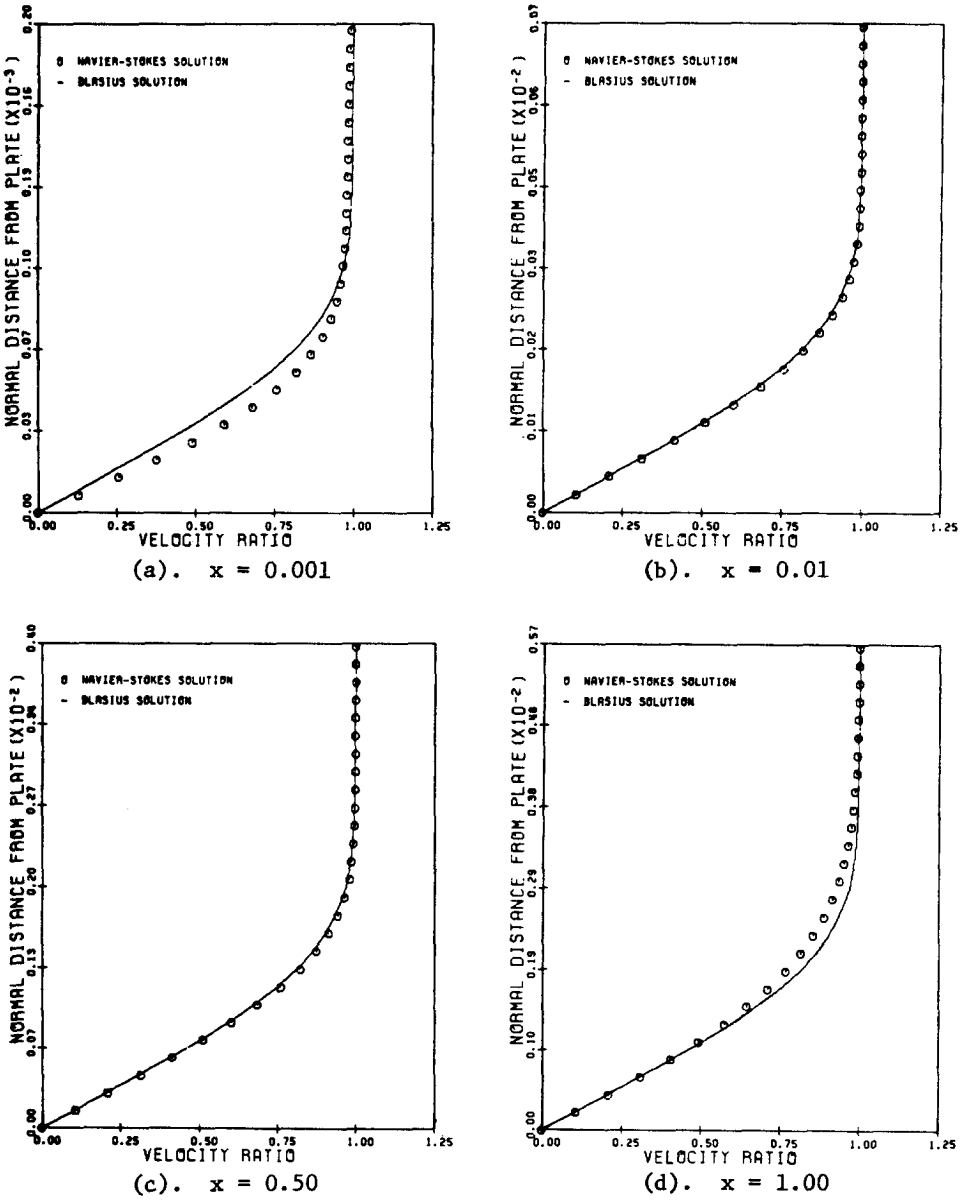

FIG. 5. Semi-infinite flat plate solution. $t = 1.24$. (Downstream boundary at eight times the distance where Blasius boundary layer slope is 0.01, XMAX = 0.45312).

as time increases, the agreement with the Blasius solution deteriorates as expected as this boundary is approached (position 1.0 in these figures). The loss of flow in the lower portion of the boundary layer that results from this continual thickening of the profile that occurs upstream of this boundary. The agreement with the Blasius profile in regions farther removed from the downstream boundary is good. Note that the profiles upstream cling to the Blasius as the downstream profile moves away.

Coordinate system control was used to cause the system to expand down the plate. The agreement with the Blasius solution extends very near the leading edge, since the coordinate lines are more closely spaced near the leading edge. With the Blasius boundary layer solution as the downstream boundary condition the problem becomes a steady-state problem, and the agreement with the boundary layer solution is excellent, except at the first few steps near the leading edge [31].

2. *Göttingen 625 airfoil.* The body-fitted coordinate system used in this solution is illustrated in Fig. 6. The flow Reynolds number was taken as 2000 at an angle of attack of 5 degrees. Stream function contours are illustrated shortly after the impulsive start in Fig. 7a. The starting vortex appears as the dip immediately above the trailing edge. Figure 7b also indicates that computational "wiggles" (Roache [33]) have developed in the solution near the airfoil trailing edge. The wiggles evolved due to the maintenance of zero vorticity at the airfoil trailing edge. This restriction was eventually removed and the wiggles died out. Laminar separation occurred on the

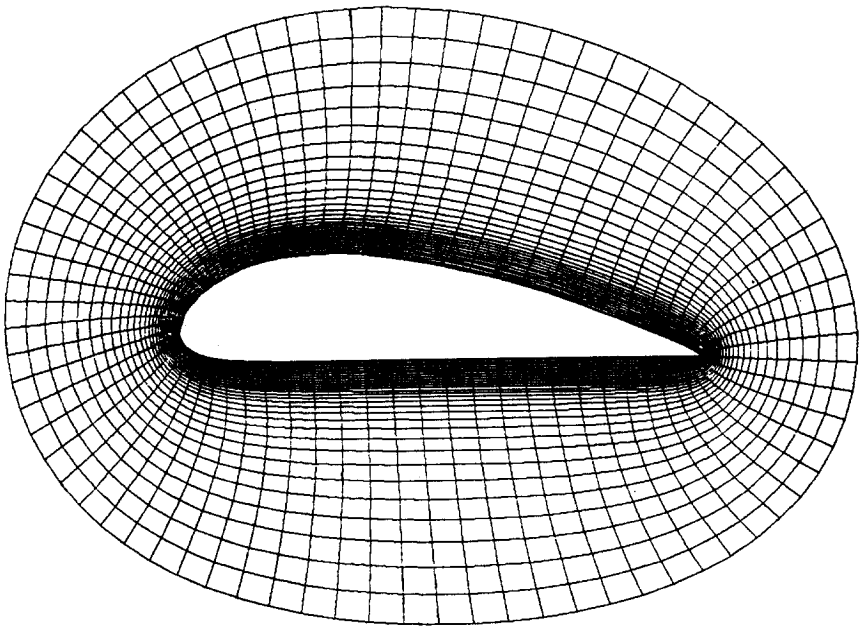

FIG. 6. Coordinate system—Göttingen 625 airfoil, attraction to body.

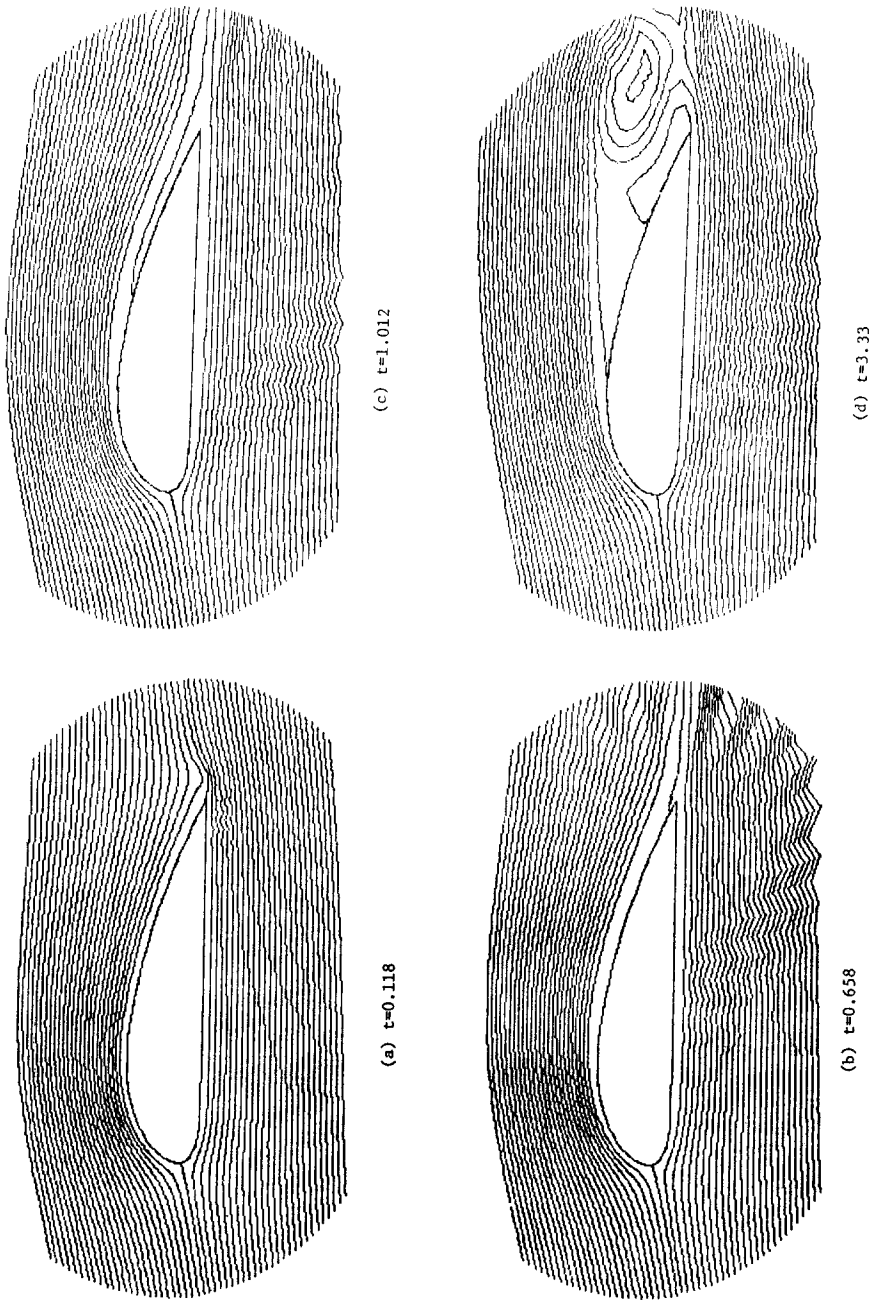

FIG. 7. ψ—Göttingen 625 airfoil.

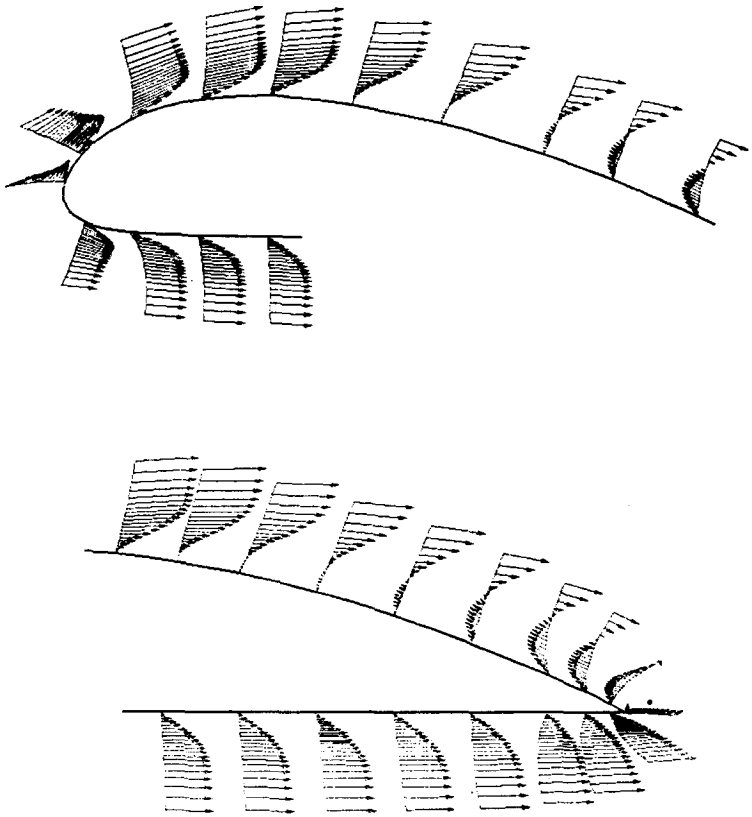

FIG. 8. Velocity profiles—Göttingen 625 airfoil; $\theta = 5°$, $R = 2000$, $t = 1.83$.

trailing edge portion of the upper surface at a time of $t = 0.658$ (Fig. 7b). The separation point moved rapidly upstream to the half-chord location accompanied by an increase in the thickness of the separated region (Fig. 7c). The separated region is clearly indicated in the velocity profiles in Fig. 8. Sample pressure distributions at two times are shown in Fig. 9. The distributions and resulting force coefficients are characteristic of friction dominated flows (Fig. 9a) and pressure losses due to flow separation as evidenced by Fig. 9b.

3. *Cambered rock.* To illustrate the ability of the body-fitted coordinate method to handle quite arbitrary geometries, the viscous flow about the cambered rock was developed at a Reynolds number of 500. The body-fitted coordinate system utilized for this solution is shown in Fig. 10. Vorticity and ψ-contours are given in Fig. 11, and velocity profiles are shown in Fig. 12. Although the accuracy of these calculations is not likely to be tested by experimental results, the flow produced by the numerical computations appears intuitively reasonable. In particular, the continued separation and reattachment which occurred in the concave regions of the body developed in a totally realistic and believable fashion.

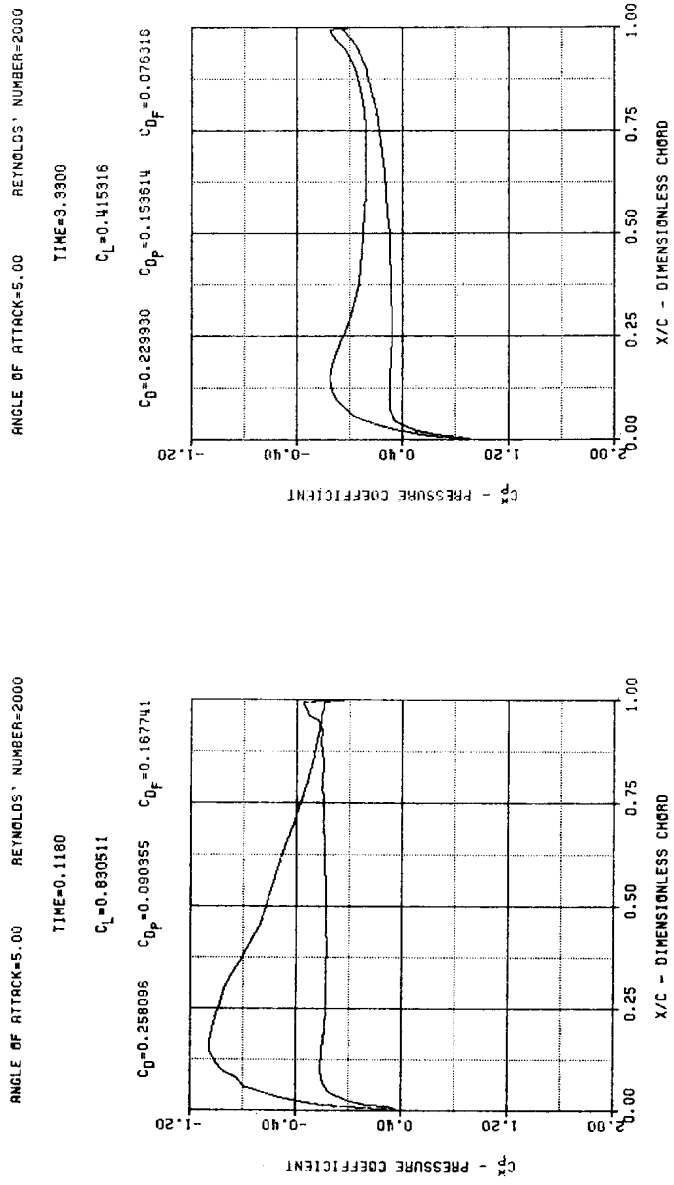

FIG. 9. Pressure distribution—Göttingen 625 airfoil.

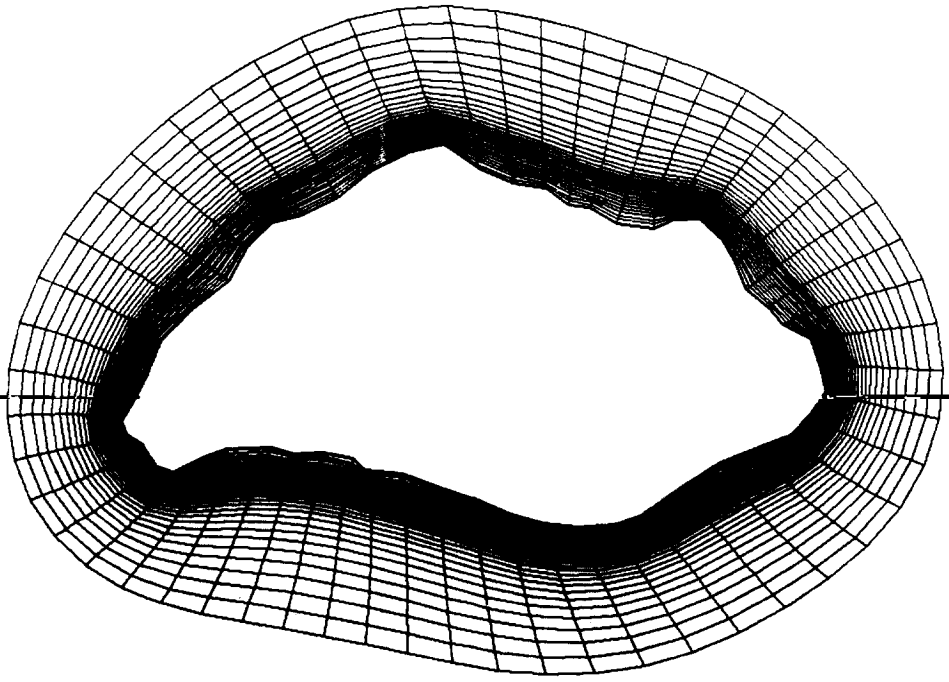

FIG. 10. Coordinate system—Cambered rock, attraction to body.

4. POTENTIAL FLOW SOLUTION

A. *Laplace Equation*

The two-dimensional irrotational flow about any number of bodies may be described by the Laplace equation for the stream function ψ

$$\psi_{xx} + \psi_{yy} = 0 \tag{10}$$

with boundary conditions

$\psi(x, y) =$ constant on each body,

$\psi(x, y) = y \cos\theta - x \sin\theta$ at infinity,

where θ is the angle of attack of the free stream relative to the positive x-axis. Here the stream function is nondimensionalized relative to the airfoil chord and the freestream velocity. When transformed to the curvilinear coordinate system this equation becomes

$$\alpha\psi_{\xi\xi} - 2\beta\psi_{\xi\eta} + \gamma\psi_{\eta\eta} + J^2[Q(\xi, \eta)\,\psi_\eta + P(\xi, \eta)\,\psi_\xi] = 0 \tag{11}$$

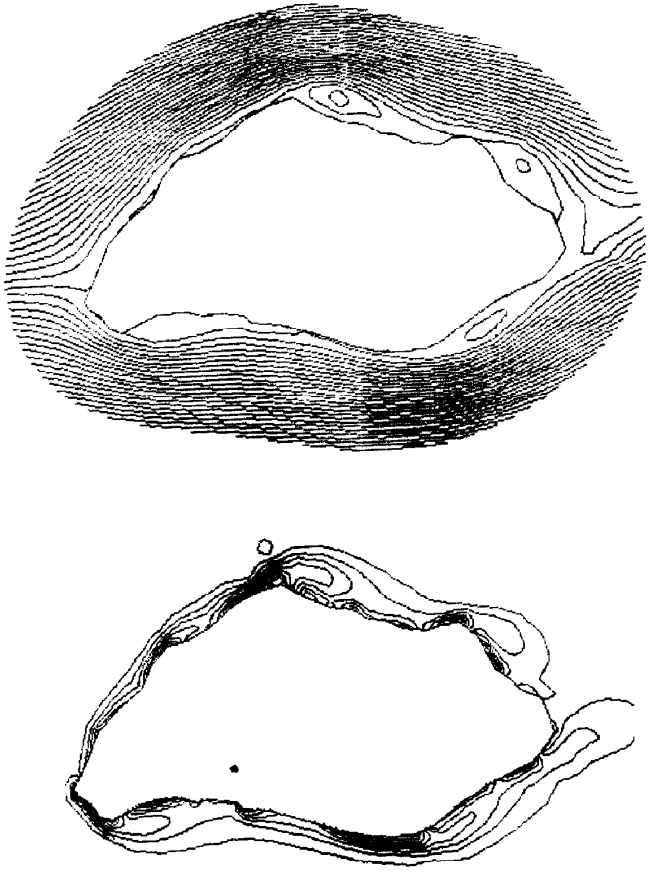

FIG. 11. ψ and ω contours—Cambered rock, $t = 0.35$.

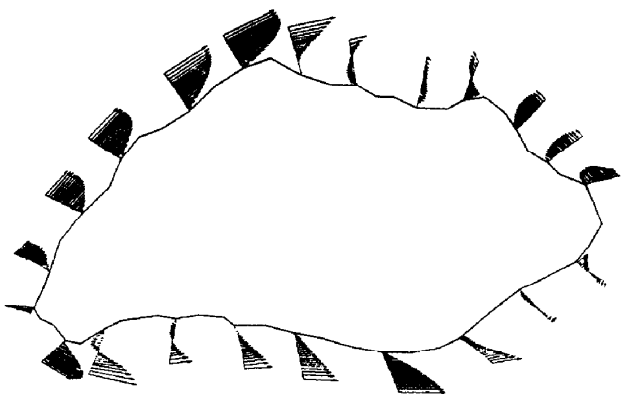

FIG. 12. Velocity profiles—Rock, $R = 500$, $t = 1.2$.

where α, β, γ, and J are given above, and the transformed boundary conditions are, for a single body,

$$\psi(\xi, \eta) = \psi_0 \qquad \text{on } \eta = \eta_1 \text{ (i.e., on } \Gamma_1^*), \tag{12a}$$

$$\psi(\xi, \eta) = y(\xi, \eta_2) \cos\theta - x(\xi, \eta_2) \sin\theta \qquad \text{on } \eta = \eta_2 \text{ (i.e., on } \Gamma_2^*). \tag{12b}$$

The uniqueness is implied by requiring that the solution be periodic in $-\infty < \xi < \infty$, $\eta_1 \leqslant \eta \leqslant \eta_2$. α, β, γ, and J are calculated during the generation of the coordinate system. Equation (11) is approximated using second-order, central differences for all derivatives, and the resulting difference equation is solved by accelerated Gauss–Seidel (SOR) iteration on the rectangular transformed field.

The solution of (11) on the transformed field is constructed in the same manner that has been previously described for the solution of (2). The single equation (11) replaces the two equations (2a) and (2b), and the boundary conditions are given by (12). The total number of difference equations thus is $I(J-1)$ for a single airfoil.

B. *Velocity*

The velocity components are calculated from the equations $u = \psi_y$, $v = -\psi_x$, which in the transformed plane become,

$$u = (x_\xi \psi_\eta - x_\eta \psi_\xi)/J, \tag{13a}$$

$$v = (y_\xi \psi_\eta - y_\eta \psi_\xi)/J. \tag{13b}$$

Velocities in the interior of the field may be obtained from these relations using second-order central difference expressions for all derivatives as given above.

On the body surface, $\psi_\xi = 0$, so that these expressions reduce to $u = x_\xi \psi_\eta / J$ and $v = y_\xi \psi_\eta / J$. Also, the unit tangent vector on the body surface is given by (see [28])

$$\boldsymbol{\tau} = (\mathbf{i} x_\xi + \mathbf{j} y_\xi)/\gamma^{1/2}. \tag{14}$$

Then the velocity component tangential to the surface is given by

$$v_t = \mathbf{v} \cdot \boldsymbol{\tau} = (u x_\xi + v y_\xi)/\gamma^{1/2} = (\gamma^{1/2}/J)\, \psi_\eta \,. \tag{15}$$

On the surface, the ξ-derivatives are approximated by the second-order central difference expressions given above, as in the interior of the field, at all points except those on the cut, $i = 1$ and $i = I$, where second-order one-sided expressions are used. Thus

$$(f_\xi)_{1,1} = \tfrac{1}{2}(-f_{3,1} + 4f_{2,1} - 3f_{1,1}), \tag{16a}$$

$$(f_\xi)_{I,1} = \tfrac{1}{2}(f_{I-2,1} - 4f_{I-1,1} + 3f_{I,1}). \tag{16b}$$

The η-derivatives on the surface are approximated at all points by second-order one-sided expressions. (First- and third-order expressions were also evaluated [34])

$$(f_\eta)_{i,1} = \tfrac{1}{2}(-f_{i,3} + 4f_{i,2} - 3f_{i,1}). \tag{17}$$

C. *Kutta Condition*

The value of the boundary value of ψ on the body, ψ_0, is determined by imposing the Kutta condition that the flow leave the sharp trailing edge of an airfoil smoothly. For a cusped trailing edge (zero included angle) this condition requires only that the velocity approach the same value at the trailing edge on the upper and lower surfaces of the airfoil. For a trailing edge with finite included angle it is required that the trailing edge be a stagnation point. It was found, however, that the requirement that the same limit be approached at the trailing edge on the upper and lower surfaces was superior numerically with both types of trailing edges [34]. This limit condition was also applied by Giesing [6] as the Kutta condition with a finite trailing edge in the potential flow solution using superposition of singularities.

In the present solution the Kutta condition thus was applied by requiring that the value of the velocity component tangential to the body surface extrapolated quadratically at the trailing edge from neighboring points on the upper surface be equal to that extrapolated from neighboring points on the lower surface. Linear and cubic extrapolations were also evaluated [34], as well as the simple requirement that the velocity vanish at the trailing edge. This application of the Kutta condition is as follows. (Here superscript 0 refers to the trailing edge, and the other superscripts to successively distant neighboring points on the body surface as illustrated in Fig. 13. These points are, of course, equispaced in the transformed plane.)

$$2v_t^{(1+)} - v_t^{(2+)} = v_t^{(0)} = 2v_t^{(1-)} - v_t^{(2-)}. \tag{18}$$

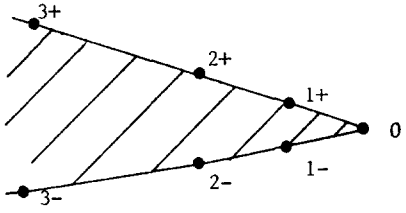

FIG. 13. Extrapolation points for application of Kutta Condition.

D. *Superposition of Solutions*

Since the system to be solved is linear in ψ, the solution for a single airfoil at any angle of attack may be obtained by superposing three component solutions: (1) a solution at 0° angle of attack with no circulation, (2) a solution at 90° angle of attack with no circulation, and (3) a solution with circulation but zero freestream velocity

as done by Giesing [6]. These three component solutions, written $\psi^{(i)}(\xi, \eta)$, $i = 1, 2, 3$, each satisfy Eq. (11), with the respective boundary conditions

$$\psi^{(1)}_{i,1} = 0, \qquad i = 1 \cdots I, \tag{19a}$$

$$\psi^{(1)}_{i,J} = y_{i,J}, \qquad i = 1 \cdots I, \tag{19b}$$

$$\psi^{(2)}_{i,1} = 0, \qquad i = 1 \cdots I, \tag{20a}$$

$$\psi^{(2)}_{i,J} = -x_{i,J}, \qquad i = 1 \cdots I, \tag{20b}$$

$$\psi^{(3)}_{i,1} = 1, \qquad i = 1 \cdots I, \tag{21a}$$

$$\psi^{(3)}_{i,J} = 0, \qquad i = 1 \cdots I. \tag{21b}$$

The complete solution with arbitrary circulation then is

$$\psi(\xi, \eta; \lambda) = \psi^{(1)}(\xi, \eta) \cos \theta + \psi^{(2)}(\xi, \eta) \sin \theta + \lambda \psi^{(3)}(\xi, \eta). \tag{22}$$

The Kutta Condition is then satisfied by choosing the coefficient λ such that (18) is satisfied, the tangential velocities being given by Eq. (15) with ψ from Eq. (22), using a one-sided difference expression analogous to Eq. (17) for the η-derivative.

Thus it is only necessary to solve the system of difference equations three times for a given airfoil. The solution at any angle of attack may then be obtained without resolving the difference system.

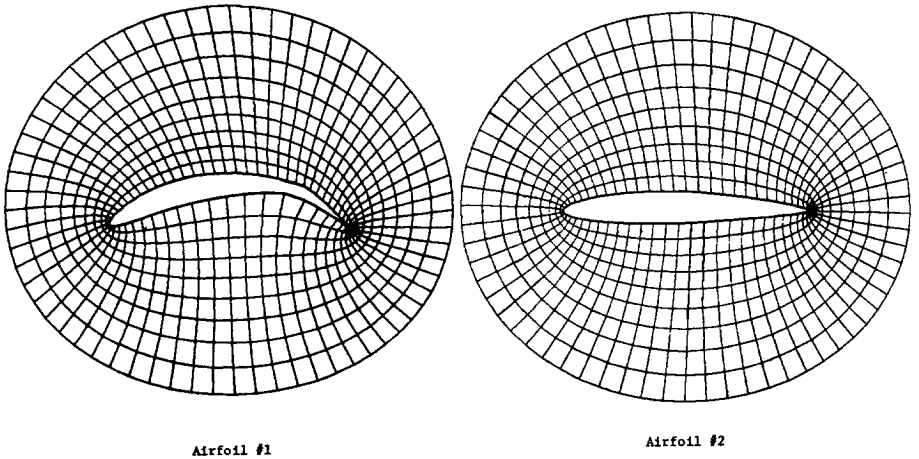

FIG. 14. Coordinate systems, Karman–Trefftz airfoils.

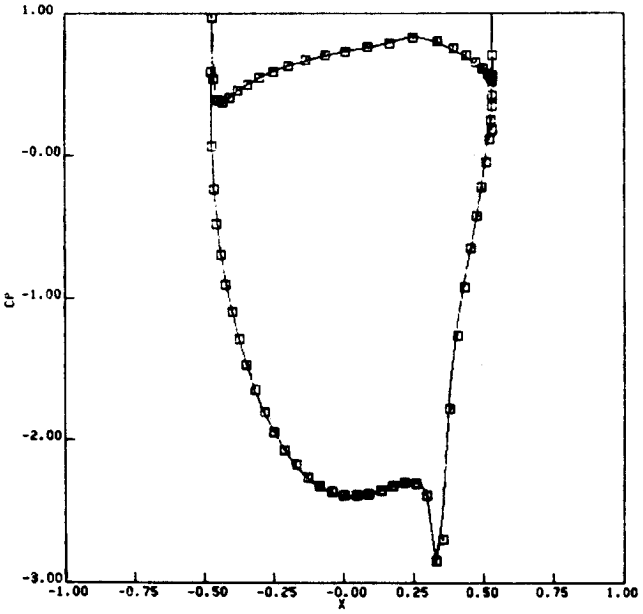

(a) Pressure Distribution

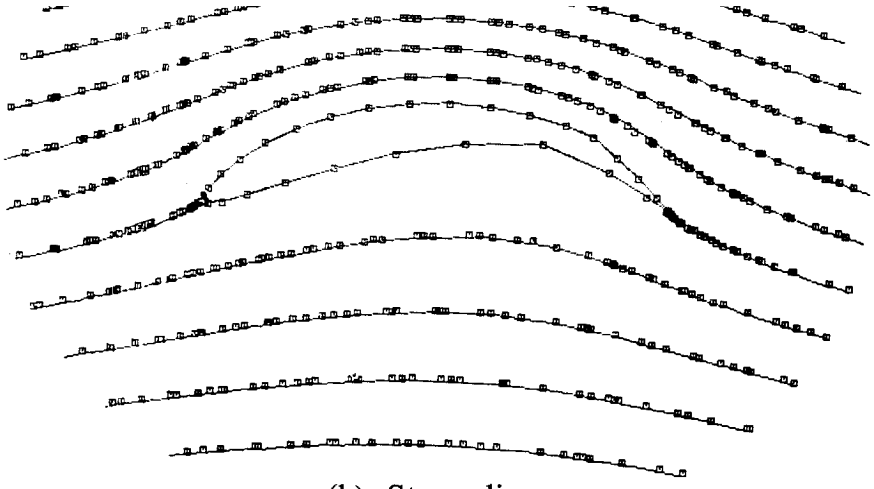

(b) Streamlines

FIG. 15. Comparison of numerical and analytical solutions—Flapped Karman–Trefftz airfoil. (Solid line is analytical; symbols are numerical.)

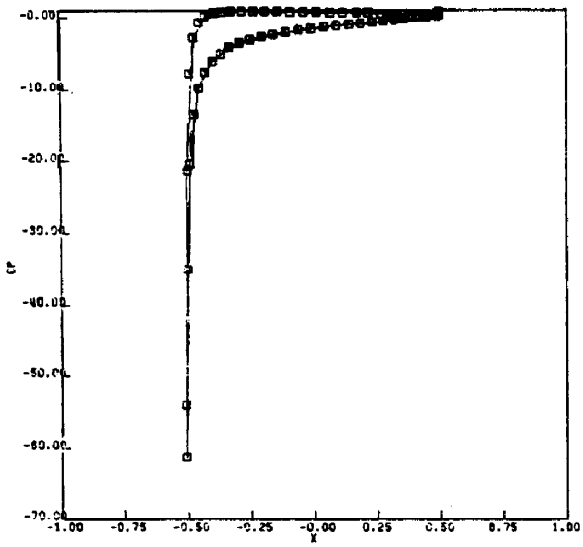

(a) Pressure Distribution

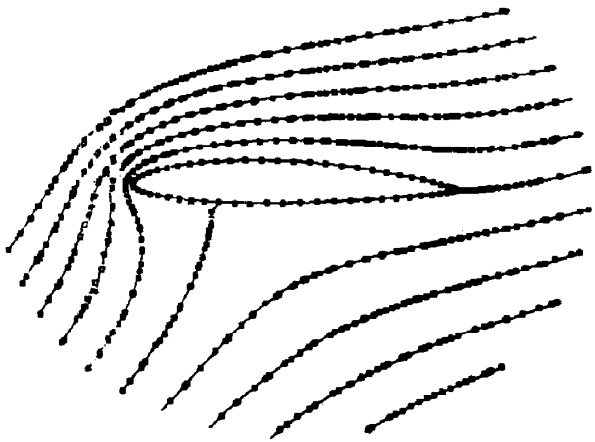

(b) Streamlines

FIG. 16. Comparison of numerical and analytical solutions–Karman–Trefftz airfoil. (Solid line is analytical; symbols are numerical.)

E. *Surface Pressure and Force Coefficients*

The pressure coefficient at any point in the field may be obtained from the velocities via the Bernoulli equation, which in the present nondimensional variables is

$$C_p = 1 - |\mathbf{v}|^2. \tag{23}$$

On the body surface this becomes, from (15),

$$C_p = 1 - (\gamma/J^2)\,\psi_\eta^2 \tag{24}$$

with the derivative evaluated by the difference expression (17). The nondimensional force on the body is given by (9) with zero ω.

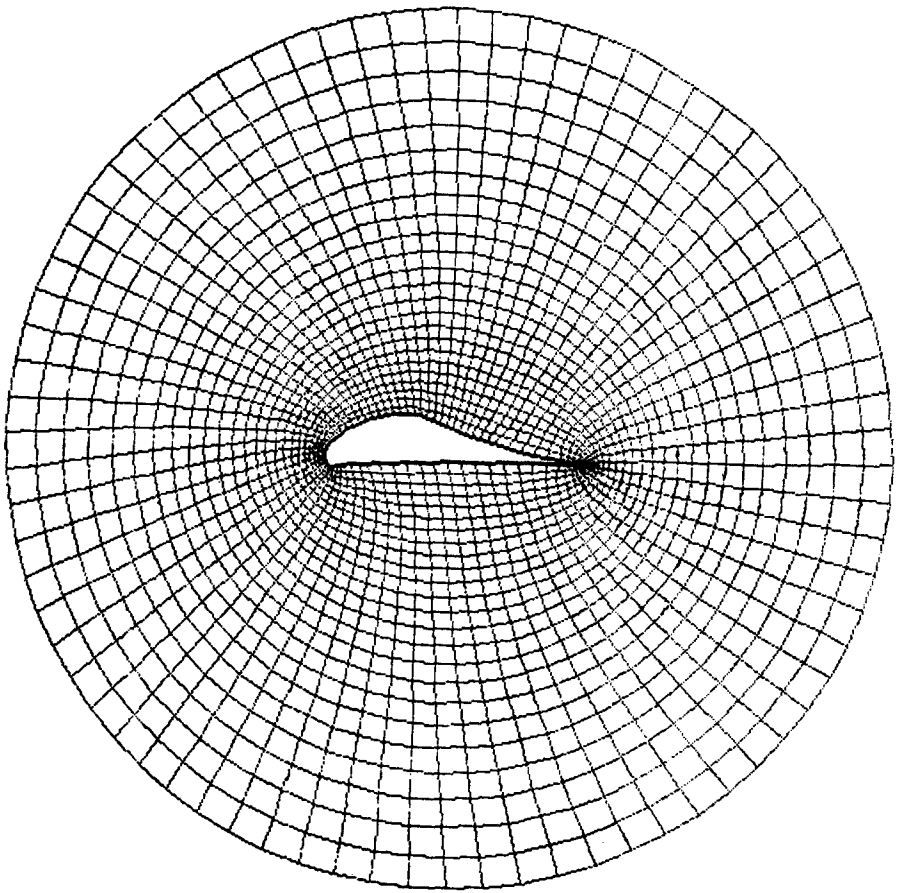

FIG. 17. Coordinate system—Liebeck laminar airfoil.

The integrals can be evaluated by numerical quadrature using either the trapezoidal rule or Simpson's rule, both of which were evaluated during the course of the investigation [34]. The former was found to be sufficient

$$\oint f\,d\xi = \tfrac{1}{2}(f_{1,1} + f_{I,1}) + \sum_{i=2}^{I-1} f_{i,1}\,. \tag{25}$$

F. *Results*

An extensive study was made to determine the effects of the various parameters involved on the accuracy of the numerical solution [34]. Numerical results for the lift and drag coefficients, the surface pressure distribution, and the stream function contours for two Karman–Trefftz airfoils were compared with the analytic solutions [35] using several values for each of the parameters that must be chosen in the numerical solution.

Coordinate systems for these two airfoils are given in Fig. 14 and typical comparisons with the analytic solution are given in Figs. 15 and 16. A comparison of the potential flow solution with experimental results for a Liebeck laminar airfoil [36] is also given in Fig. 18, the coordinate system being given in Fig. 17.

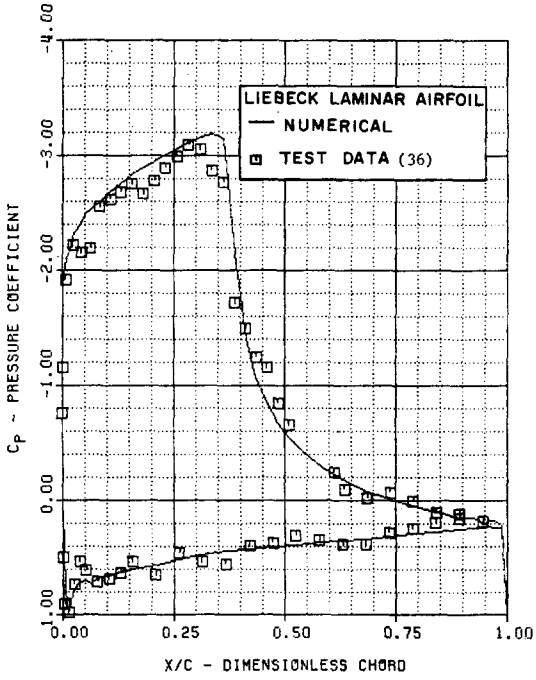

FIG. 18. Comparison of experimental and numerical potential flow results—Liebeck laminar airfoil.

5. Conclusions

The use of body-fitted curvilinear coordinate systems allows numerical flow solutions for fields containing any number of bodies of arbitrary shape to be produced by finite-difference methods essentially as easily as that about single simple bodies. The computer code is not dependent on either the number or the shapes of the bodies, so that different bodies can be treated by simple changes in the input.

The ability of the coordinate system method to compact the radial mesh spacing near the body allowed solutions to the viscous flow equations in which accurate pressure and force coefficients could be calculated. The approach of iterating for the boundary vorticity to explicitly enforce the no-slip condition, along with the inherent stability of implicit methods, permitted solutions at moderate Reynolds numbers. Minor improvements in the boundary vorticity iteration should result in accurate solutions up to the transition Reynolds number for a given flow. Recent progress has been made in this area. The body-fitted coordinates are currently being used to obtain solutions of turbulent flows, transonic flows, and flows with free surfaces. The procedure is also applicable to fields with more than one body, and viscous solutions for multiple airfoils are presently under development.

References

1. U. B. Mehta and Z. Lavan, "Starting Vortex, Separation Bubbles and Stall—A Numerical Study of Laminar Unsteady Flow Around an Airfoil," AFOSR-TR-73-0640 (1972). (Available from DDC as AD 758 831.)
2. C. Dawson and M. Marcus, DMC—A computer code to simulate viscous flow about arbitrary shaped bodies, *in* "Proceedings of the 1970 Heat Transfer and Fluid Mechanics Institute," pp. 323–338, 1970.
3. R. Meyder, Solving the conservation equations in fuel rod bundles exposed to parallel flow by means of curvilinear-orthogonal coordinates, *J. Computational Phys.* **17** (1975), 53.
4. T. Gal-Chen and R. C. J. Somerville, On the use of a coordinate transformation for the solution of the Navier–Stokes equations, *J. Computational Phys.* **17** (1975), 209.
5. T. Gal-Chen and R. C. J. Somerville, Numerical solution of the Navier–Stokes equations with topography, *J. Computational Phys.* **17** (1975), 276.
6. J. P. Giesing, "Potential Flow About Two-Dimensional Airfoils," Rept. LB 31946, Douglas Aircraft Co., 1965.
7. J. L. Hess and A. M. O. Smith, Calculation of potential flow about arbitrary bodies, *in* "progress in Aeronautical Sciences," Vol. 8, p. 1, Pergammon Press, Oxford, 1966.
8. J. P. Giesing, Nonlinear two-dimensional unsteady potential flow with lift, *J. Aircr.* **5** (1968), 135.
9. J. L. Hess, "Calculation of Potential Flow About Arbitrary Three-Dimensional Lifting Bodies," Rept. MDC J5679-01, McDonnel Douglas Corp., 1972.
10. R. H. Djojodihardjo and S. E. Widnall, A numerical method for the calculation of nonlinear, unsteady lifting potential flow problems, *AIAA J.* **7** (1969), 2001.
11. E. Grodtkjaer, A direct integral equation method for the potential flow about arbitrary bodies, *Int. J. Numer. Methods Eng.* **6** (1973), 253.
12. W. C. Webster, The flow about arbitrary, three-dimensional smooth bodies, *J. Ship Res.* **19** (1975), 206.
13. L. J. Doctors, An application of the finite element technique to boundary value problems of potential flow, *Int. J. Numer. Methods Eng.* **2** (1970), 243.

14. J. H. ARGYRIS AND G. MARUZEK, Potential flow analysis by finite elements, *Ing. Arch.* **41** (1972), 1.
15. U. MEISSNER, A mixed finite element model for use in potential flow problems, *Int. J. Numer. Methods Eng.* **6** (1973), 467.
16. T. THEODORSEN AND I. E. GARRICK, "General Potential Theory of Arbitrary Wing Sections,"
17. D. C. IVES, A modern look at conformal mapping, including doubly connected regions, *AIAA J.* **14** (1976), 1006.
18. J. F. THOMPSON, F. C. THAMES, AND C. W. MASTIN, Automatic numerical generation of body fitted curvilinear coordinate system for field containing any number of arbitrary two-dimensional bodies, *J. Computational Phys.* **15** (1974), 299.
19. A. J. WINSLOW, Numerical solution of the quasi-linear Poisson equation in a non-uniform triangular mesh, *J. Computational Phys.* **2** (1966), 149.
20. W. D. BARFIELD, An optimal mesh generator for Lagrangian hydrodynamic calculations in two space dimensions, *J. Computational Phys.* **6** (1970), 417.
21. W. H. CHU, Development of a general finite difference approximation for a general domain, Part I. Machine transformation, *J. Computational Phys.* **8** (1971), 392.
22. A. A. AMSDEN AND C. W. HIRT, A simple scheme for generating general curvilinear grids, *J. Computational Phys.* **11** (1973), 348.
23. S. K. GODUNOV AND G. P. PROKOPOV, The use of moving meshes in gas dynamics computations, *U.S.S.R. Comput. Math. and Math. Phys.* **12** (1972), 182.
24. G. STADIUS, "Construction of Orthogonal Curvilinear Meshes by Solving Initial Value Problems," Dept. of Computer Sciences Report No. 53, Uppsala University, Sweden, 1974.
25. F. C. THAMES, "Numerical Solution of the Incompressible Navier–Stokes Equations about Arbitrary Two-Dimensional Bodies," Ph.D. Dissertation, Mississippi State University, 1975.
26. J. F. THOMPSON, F. C. THAMES, C. W. MASTIN, AND S. P. SHANKS, Use of numerically generated body-fitted curvilinear coordinate systems for solution of the Navier–Stokes equations, *in* "Proceedings of the AIAA 2nd Computational Fluid Dynamics Conference," Hartford, Conn., 1975.
27. F. C. THAMES, J. F. THOMPSON, AND C. W. MASTIN, Numerical solution of the Navier–Stokes equations for arbitrary two-dimensional airfoils, *in* "Proceedings of NASA Conference on Aerodynamic Analyses Requiring Advanced Computers," Langley Research Center, NASA SP-347 (1975).
28. J. F. THOMPSON, F. C. THAMES, AND C. W. MASTIN, "Boundary-Fitted Curvilinear Coordinate Systems for Solution of Partial Differential Equations on Fields Containing Any Number of Arbitrary Two-Dimensional Bodies," NASA CR-2729 (1976).
29. M. ISRAELI, "A Fast Implicit Method for Time Dependent Viscous Flows," *Stud. Appl. Math.* **49** (1970), 327.
30. R. ARIS, "Vectors, Tensors, and Basic Equations of Fluid Mechanics," Prentice–Hall, Englewood Cliffs, N. J. 1962.
31. R. L. WALKER, "Numerical Solution of the Navier-Stokes Equations for Incompressible Viscous Laminar Flow Past a Semi-Infinite Flat Plate," M.S. Thesis, Mississippi State University, 1974.
32. H. SCHLICHTING, "Boundary Layer Theory," 4th ed., McGraw–Hill, New York, 1960.
33. P. J. ROACHE, "Computational Fluid Dynamics," Hermosa Publishers, Albuquerque, New Mexico, 1972.
34. J. F. THOMPSON AND F. C. THAMES, "Numerical Solution of Potential Flow About Arbitrary Two-Dimensional Bodies," NASA CR, to be released in 1976.
35. K. KARAMACHETI, "Principles of Ideal-Fluid Aerodynamics," Wiley, New York, 1966.
36. R. H. LIEBECK, "Wind Tunnel Tests of Two Airfoils Designed for High Lift Without Separation in Incompressible Flow," McDonnel Douglas Corp., Report No. MDC-J5667/01 (1972).